SIMULATION OF MARINE LATENT HEAT FLUXES IN THE UNIFIED MODEL

John M. Edwards *

1. INTRODUCTION

Evaporation from the oceans is an important process in both the atmospheric hydrological and energy cycles and climatologies of latent heat fluxes are very valuable in assessing the performance of general circulations models (GCMs). Traditionally, such climatologies have been derived from measurements taken from ships (*e. g.* da Silva (1994) and the NOC1.1 climatology (Josey *et al.* 1999)). These climatological latent heat fluxes are significantly lower than those obtained from GCMs: in the case of the latest climate configuration of the Met Office's climate model (HadGAM1, Martin *et al.* 2006), the discrepancy in the global annual mean oceanic latent heat flux is around 30 Wm^{-2}.

A more recent satellite-based climatology, GSSTF2.0 (Chou *et al.* 2003, Chou *et al.* 2004), gives latent heat fluxes which are around 15 Wm^{-2} higher in the global annual mean than the ship-based climatologies. This climatology has been compared more extensively with field observations and the authors conclude that the GSSTF2.0 fluxes are probably more reliable than earlier estimates, although regional biases still exist. An independent study (Grist and Josey 2003), in which the fluxes in the NOC1.1 climatology were adjusted to balance estimates of oceanic heat transports, also suggested that the latent heat flux in the NOC1.1 climatology needed to be increased by around a similar amount to balance the oceanic flux budget. These adjusted fluxes are known as the NOC1.1a climatology.

Higher latent heat fluxes would substantially reduce the discrepancy between the model and the climatologies and it seems appropriate to reassess the model's simulation of the latent heat flux in the light of these new climatological estimates. First, however, we ask how consistent climatologies of latent heat fluxes are with other flux climatologies within the context of the atmospheric hydrological and energy cycles.

*Corresponding author address: John M. Edwards, Met Office, Exeter, Devon, EX1 3PB, U.K.; email:john.m.edwards@metoffice.com

2. CONSISTENCY OF CLIMATOLOGIES

Integrating the equation for the conservation of water substance over the depth of the atmosphere, from the height of the surface H_s to the top of the atmosphere H_T, and over a period of time $\mathcal{T}$, the hydrological cycle can be written as

$$\begin{aligned} R_{\mathrm{hyd}} &= L(\bar{E}-\bar{P}) - \overline{\nabla_H . \int_{H_s}^{H_T} \rho q \mathbf{v}\, dz} \\ &- \frac{1}{\mathcal{T}}\Delta \int_{H_s}^{H_T} \rho q\, dz \end{aligned} \quad (1)$$

where R_{hyd} is the residual in the hydrological cycle, L is the latent heat of vaporization of water, E is the rate of evaporation, with the overbar denoting an average in time, P is the rate of precipitation, ρ is the atmospheric density and q the specific humidity, while Δ denotes the increment over the period $\mathcal{T}$. For a long-term annual mean the final tendency term will vanish, but it is required in forming seasonal budgets. If perfect climatologies were available for each term in this budget, the residual would vanish.

Similarly, the total energy density in the atmosphere is the sum of the internal, kinetic potential and latent energies, $c_V T + (1/2)\mathbf{v}^2 + \Phi + Lq$, where c_V is the specific heat capacity of air at constant volume, T is the temperature, $\mathbf{v}$ is the velocity and Φ is the geopotential. The budget of total energy can be written as

$$\begin{aligned} R_{\mathrm{en}} &= \bar{F}_{\mathrm{lat}} + \bar{F}_{\mathrm{sens}} + \bar{F}_{\mathrm{rad}} \\ &- \overline{\nabla_H . \int_{H_s}^{H_T} \rho \mathbf{v} \left(c_P T + \frac{1}{2}\mathbf{v}^2 + \Phi + Lq \right) dz} \\ &- \frac{1}{\mathcal{T}}\Delta \int_{H_s}^{H_T} \rho \left(c_V T + \frac{1}{2}\mathbf{v}^2 + \Phi + Lq \right) dz \end{aligned} \quad (2)$$

Here F_{lat} and F_{sens} are the latent and sensible heat fluxes into the atmosphere at the surface and F_{rad} is the net radiative flux into the atmospheric column, which may be written in the form

$$F_{\mathrm{rad}} = S_t^{\downarrow} - S_t^{\uparrow} - S_s^{(N)} - L_t^{\uparrow} - L_s^{(N)}, \quad (3)$$

where the terms on the right represent respectively the incident solar flux at the top of the atmosphere,

the reflected shortwave flux at the top of the atmosphere, the net shortwave flux at the surface, the outgoing longwave flux, and the net longwave flux at the surface. Again, if the climatologies were perfect $R_{\rm en}$ would vanish. (For a full discussion of these budgets see *e. g.* Trenberth *et al.* (1991), Trenberth and Caron (2001) and the references therein.)

A study of the consistency of climatologies was carried out by Yu *et al.* (1999), who performed a zonal annual mean analysis, taking the fluxes at the earth's surface and at the top of the atmosphere from the climatologies available at the time and divergences from a reanalysis. To form zonal averages, they also required latent and sensible heat fluxes over land, which the took from the reanalysis. They suggested that the hydrological cycle was in balance, but that there was an imbalance in the total energy cycle of around 20 Wm^{-2}, which might be due to an underestimate of shortwave absorption in the radiation model used to derive the climatological surface radiative fluxes from satellite observations at the top of the atmosphere. (They considered the empirically derived radiative fluxes contained in the ship-based climatologies unreliable.) With the appearance of several new climatologies, not only of latent heat fluxes, but also of precipitation and radiative fluxes, it is important to review the question of consistency. In contrast to the study of Yu *et al.* (1999), we shall not form zonal means, thus avoiding the need for sensible and latent heat fluxes over land, and will also examine seasonal patterns in the energy cycle.

As an example of the application of this analysis to the hydrological cycle, figure 1 shows the annual mean residual in the hydrological cycle from two different combinations of climatologies. In the upper panel, the latent heat fluxes are taken from the GSSTF2.0 climatology and the precipitation from the CMAP climatology (Xie and Arkin 1997), while the divergences of moisture are taken from the ERA-40 reanalysis. There are large residuals over and around the maritime continent. These can be related to a known moist bias in the specific humidity at 10 m in the GSSTF2.0 climatology in these regions (implying lower latent heat fluxes), combined with an overestimate of precipitation in the CMAP climatology (Yin 2004). Other areas of significant residuals indicate regions where at least one of the climatological terms is not well characterized. The lower panel shows the residuals with precipitation taken from the GPCP2 climatology (Adler 2003) and the latent heat fluxes from the (adjusted) NOC1.1a climatology. In the mid-latitudes, the residuals are very much reduced, although there are localized imbalances along

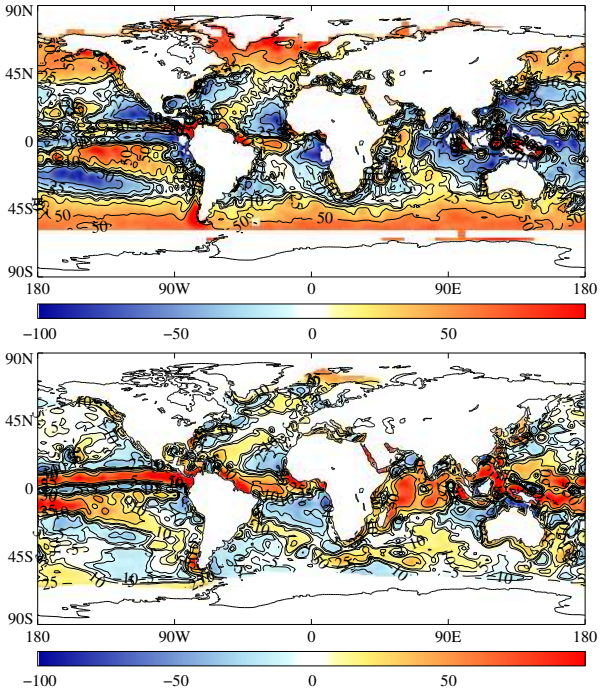

Figure 1: The residuals in the hydrological cycle (Wm^{-2}) with two different choices of climatologies. Upper panel: With divergences taken from the ERA-40 reanalysis, precipitation from the CMAP climatology and latent heat fluxes from the GSSTF2.0 climatology. Lower panel: With divergences taken from the ERA-40 reanalysis, precipitation from the GPCP2 climatology and latent heat fluxes from the NOC1.1a climatology.

the ITCZ, indicating a deficiency either in the precipitation climatology, or in the moisture divergence.

Turning to the energy cycle, figure 2 shows the residuals obtained taking divergences from the ERA-40 reanalysis, latent heat fluxes from the NOC1.1a climatology, sensible heat fluxes from the GSSTF2.0 climatology and radiative fluxes from the ISCCP-FD climatology (Zhang 2004). In most regions, the residual is negative indicating a net loss of energy from the atmosphere. The lower panels show the residuals for the northern winter and summer respectively, including the tendency terms. If the imbalances were due solely to a poor characterization of shortwave absorption in the atmosphere, significantly lower residuals would be expected in the winter hemisphere, but there is no strong seasonal cycle, suggesting that errors in other fluxes are also significant. The large residuals off the eastern edges of continents in the northern winter are particularly interesting and may indicate an underestimate of the turbulent fluxes in conditions of cold air outbreaks.

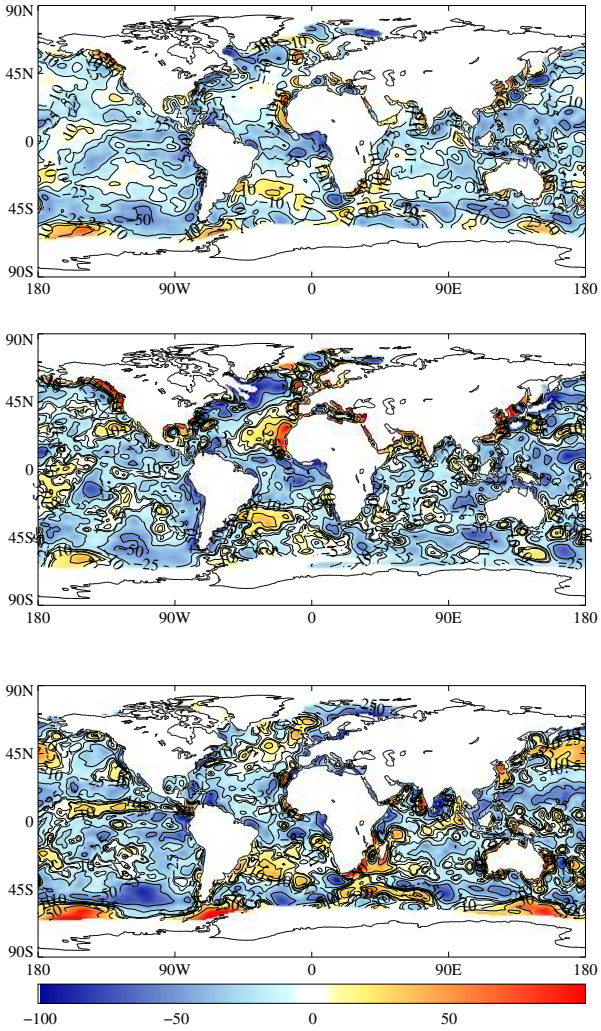

Figure 2: The residuals in the atmospheric energy cycle (Wm^{-2}) obtained with divergences taken from the ERA-40 reanalysis, latent heat fluxes from the NOC1.1a climatology, sensible heat fluxes from the GSSTF2.0 climatology and radiative fluxes from the ISCCP-FD climatology. Upper panel: Annual mean. Middle panel: December–February. Lower panel: June–August.

Cloud-base heights in the ISCCP-FD climatology are known to be low in humid conditions (Wang et al. 2000), and this may contribute to excessive downward longwave fluxes reaching the surface.

The higher latent heat fluxes of the GSSTF2.0 and NOC1.1a climatologies substantially reduce the mean bias in the energy cycle, relative to previous climatologies of latent heat fluxes and reverse the bias in the hydrological cycle, which now shows a

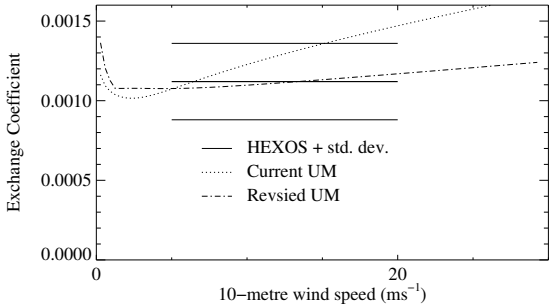

Figure 3: The neutral exchange coefficient for moisture as given by the HEXOS data (DeCosmo 1996), showing the range of those data, and as calculated using the current parametrization in the UM and the revised scheme described in the text.

net deficit in precipitation over the oceans. Overall, the regional pattern of the NOC1.1a climatology is more consistent with other climatologies than that obtained with the GSSTF2.0 climatology.

3. LATENT HEAT FLUXES IN THE UNIFIED MODEL

The GSSTF2.0 and NOC1.1 climatologies contain not only sensible and latent heat fluxes, but also the wind speeds and humidities used to derive these fluxes using bulk flux formulae:

$$H/(\rho c_P) = C_H W_{10}(\theta_s - \theta_{10}) \quad (4)$$

$$E/\rho = C_E W_{10}(\sigma q_{\rm sat}(T_s) - q_{10}), \quad (5)$$

where H is the sensible heat flux, E the rate of evaporation, with C_H and C_E as the corresponding exchange coefficients; w_{10} is the 10-m wind speed, θ_s and θ_{10} are the potential temperatures at the surface and at 10 m respectively, q_{10} is the specific humidity at 10 m, $q_{\rm sat}(T_s)$ is the saturated specific humidity at the surface temperature, T_s, and σ represents the effect of salinity in reducing the vapour pressure over the sea: in practice it can be taken as 0.98.

Two deficiencies were found in the current parametrization in the UM. Firstly, σ is omitted. Secondly, and more significantly, the use of a constant roughness length for heat and moisture leads to a significant increase in the neutral exchange coefficient for moisture with wind speed. However, recent field experiments, such as the HEXOS campaign (DeCosmo *et al.* 1996), show that there is very little change in the neutral exchange coefficient

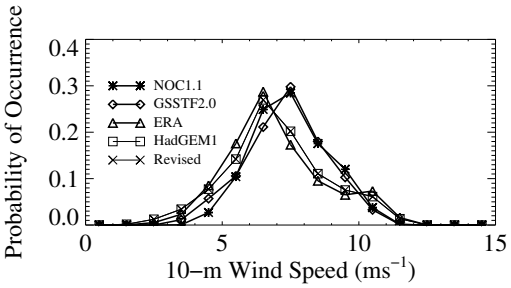

Figure 4: Histograms of the annual mean 10-m wind speeds over the oceans from the GSSTF2.0 and NOC1.1 climatologies, the ERA-40 reanalysis and the two climate integrations of the UM.

with wind-speed over the range 5–20 ms^{-1}. Figure 3 shows the mean and standard deviations of the HEXOS results. At high wind speeds, the current parametrization of the exchange coefficient gives excessive values. A revised parametrization of the thermal roughness length, making $z_{0T,q}$ inversely proportional to z_{0m} (except at low wind speeds when the surface becomes aerodynamically smooth) has been implemented. This is based on Csanady's (2001) arguments in favour of surface divergence theory and gives a much smaller increase in the exchange coefficient with wind speed. It has been calibrated to give $C_E = 0.0011$ at 10 ms^{-1}, based on the HEXOS data. The impact of this revision is described below. The exchange coefficients used in the climatological bulk formulae are closer to the HEXOS means, and as will be seen, errors in the humidity are a more significant cause of discrepancies between the climatologies than differences between the bulk flux formulae, a fact already noted by Chou *et al.* (2004).

Data from the UM used in the following comparisons come from two parallel ten-year climate integrations of the latest climate version of the UM (HadGAM1, Martin *et al.* 2006), one being the standard version of this model and the other containing the revised formulation for marine surface transfer discussed above.

3.1 10-m Winds

Figure 4 shows histograms of the 10-m wind speed from the two climatologies, the ERA-40 reanalysis and the two versions of the UM. There is a clear split between the climatologies and the model products, with the revised parametrization having little impact on the wind speeds. Maps of the differences between the climatologies and the model products show the the modelled winds are lower in the subtropics.

3.2 The Specific humidity difference

The latent heat flux depends on the difference between the specific humidity at the surface (allowing for the effect of salinity) and at 10 m. In the annual mean sense, the maximum value of this difference is around 8 gkg^{-1}. The upper panel of figure 5 shows the difference in this quantity between the NOC1.1 and the GSSTF2.0 climatologies. The GSSTF2.0 climatology is known to be too moist in the deep tropics (Chou *et al.* 2004) at 10 m, while at most other latitudes the NOC1.1 climatology is the moister. Given the suspected low latent heat fluxes in the unadjusted NOC1.1 climatology, this may indicate that there is a moist bias in the specific humidity at 10 m in the original NOC1.1 climatology. The climatologies are so different in this field that it is not possible to make a definitive statement about the systematic error in the model in this field. The revised parametrization increases this difference (lower panel) as the result of a reduction in the specific humidity at 10 m.

3.3 The Latent Heat Fluxes

Figure 6 shows a comparison of the zonal annual mean latent heat fluxes between the model and the climatologies. The standard version of HadGAM1 shows the highest latent heat fluxes and the revised parametrization reduces them slightly. The lowest fluxes are those from the original ship-based climatologies. The adjusted latent heat fluxes in the NOC1.1a climatology are generally close to the GSSTF2.0 fluxes. The known biases in the latter climatology are towards low latent heat fluxes around the equator and towards higher fluxes towards the poles. This is in agreement with the suggestion from the analysis of consistency above that the regional pattern of the NOC1.1a climatology is probably better than that in the GSSTF2.0 climatology.

3.4 Impact of the revised parametrization on other fields

The reduction of the latent heat flux with the revised parametrization leads to a reduction in overall precipitation, although, as figure 7 shows, precipitation near the equator is increased: this is actually associated with a narrowing of the ITCZ. In the mid-latitudes, the model agrees well with the GPCP2 climatology and the revised parametrization slightly improves the agreement. However, at low latitudes, the

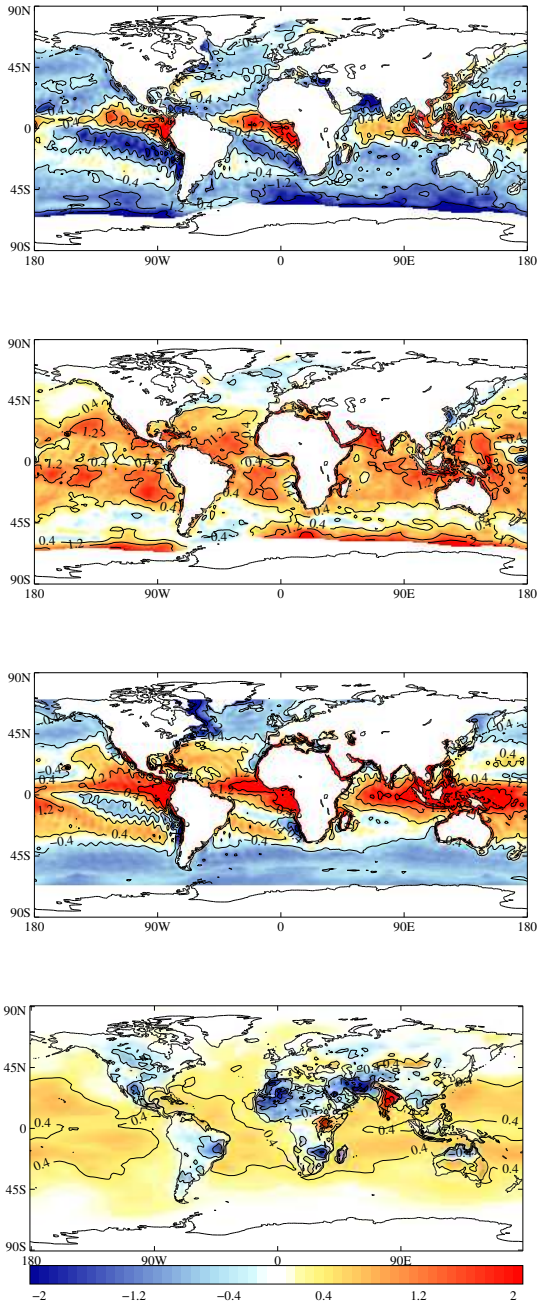

Figure 5: Comparison of the difference in the specific humidity between the surface and 10 m. Top: The difference between the NOC1.1 and GSSTF2.0 climatologies. Upper Middle: The difference between HadGAM1 and the NOC1.1 climatology. Lower Middle: The difference between HadGAM1 and the GSSTF2.0 climatology. Bottom: The impact of the revsied parametrization.

precipitation in the model is excessive even with the revised parametrization. The revised parametrization

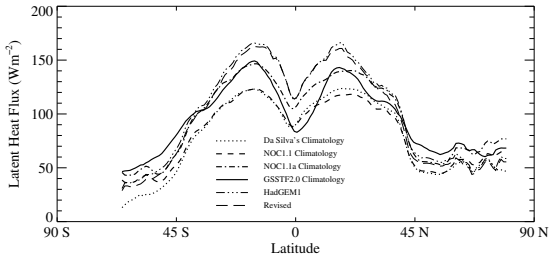

Figure 6: Comparison of the zonal annual mean latent heat fluxes between the model and the climatologies.

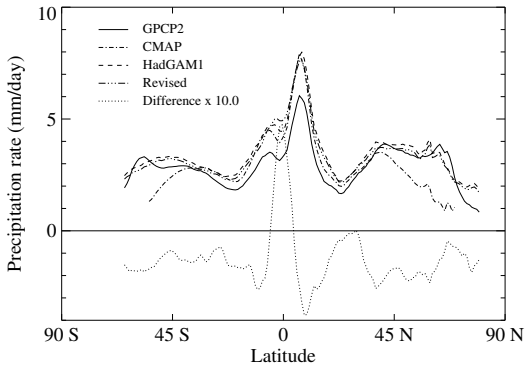

Figure 7: The zonal annual mean precipitation rate over the oceans from the CMAP and GPCP2 climatologies and from the standard and revised versions of the UM, together with the impact of the revised parametrization on an exaggerated scale.

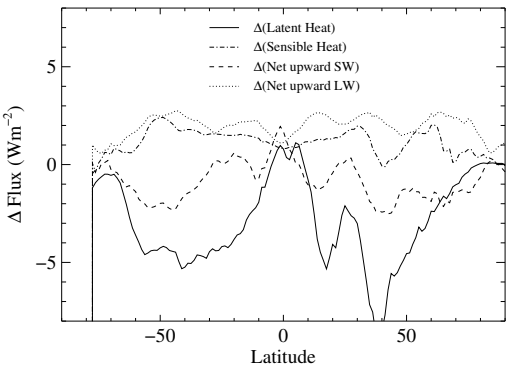

Figure 8: The impact of the revised parametrization on the zonal annual mean surface energy budget at ocean points.

also alters the surface energy budget, which is shown as a zonal annual mean over ocean points in figure 8. The reduced flux of moisture from the surface results in a cooling and drying of the atmosphere: the cooling results in an increase in the sensible heat flux, whilst the cooling and drying together result in a reduction in the downward longwave flux at the surface, increasing the net upward flux there. Conversely, the downward shortwave flux at the surface is increased.

4. CONCLUSIONS

The increased latent heat flux suggested by the new GSSTF2.0 climatology significantly reduces the imbalance in the atmospheric energy cycle, but an analysis of consistency with the hydrological cycle suggests that this climatology may underestimate the zonal variation of the latent heat flux and that the regional pattern of the adjusted NOC1.1a climatology is more realistic. A high measure of consistency in the representation of the hydrological cycle in the mid-latitudes is found with the GPCP2 and NOC1.1a climatologies. Imbalances of 10–15 Wm^{-2} still persist in the energy cycle when radiative absorption is taken from the ISCCP-FD climatology, but a seasonal analysis suggests that these cannot be explained solely in terms of a deficit in shortwave absorption.

A revision to the parametrization of oceanic evaporation in the UM brings the neutral exchange coefficient for moisture into closer agreement with field observations, reducing the model's latent heat fluxes and cooling and drying the atmosphere.

As a consequence of revisions to the climatologies and changes to the parametrization in the model, the discrepancy between the model and observations is reduced from O(30) Wm^{-2} to O(10) Wm^{-2}.

A more extensive version of this study has been prepared with a view to publication.

5. ACKNOWLEDGEMENTS

ECMWF ERA-40 data used in this study were obtained from the ECMWF data server. The GSSTF2.0 climatology was obtained from the Distributed Active Archive Centre (DAAC) `http://-daac.gsfc.nasa.gov`. The NOC climatology was obtained from the National Occeanography Centre's web-site at `http://www.noc.soton.ac.uk/-JRD/MET/fluxclimatology.html`. SRB data were obtained from the the NASA Langley Research Center Atmospheric Sciences Data Center `http://-eosweb.larc.nasa.gov`.

6. REFERENCES

R. F. Adler, G. J. Huffman, A. Chang, R. Ferraro, P.-P. Xie, J. Janowiak, B. Rudolf, U. Schneider, S. Curtis, D. Bolvin, A. Gruber, J. Susskind, P. Arkin and E. Nelkin, 2003: The version-2 global precipitation climatology project (GPCP) monthly precipitation analysis (1979-present). *J. Hydromet.*, **4**, 1147–1167

S.-H. Chou, E. Nelkin, J. Ardizzone, R. Atlas and C.-L. Shie, 2003: Surface turbulent heat and momentum fluxes over global oceans based on the Goddard satellite retrievals, version 2 (GSSTF2). *J. Climate*, **16**, 3256–3273

S.-H. Chou, E. Nelkin, J. Ardizzone, R. Atlas, 2004: A comparison of latent heat fluxes over global oceans from four flux products. *J. Climate*, **17**, 3973–3989

G. T. Csanady, 2001: Air-sea interaction: Laws and Mechanisms. *Cambridge University Press*

A. da Silva, A. C. Young and S. Levitus, 1994: Algorithms and Procedures. Vol. 1, Atlas of surface marine data 1994. *NOAA Atlas NESDIS 6*, 83 pages

J. DeCosmo, K. B. Katsaros, S. D. Smith, R. J. Anderson, W. A. Oost, K. Bumke and H. Chadwick, 1996: Air-sea exchange of water vapor and sensible heat: the humidity exchange over the sea (HEXOS) results *J. Geophys. Res.*, **101**(C5), 12,001–12,016

J. P. Grist and S. A. Josey, 2003: Inverse analysis adjustment of the SOC air-sea flux climatology using ocean heat transport constraints, *J. Climate*, **16**, 3274–3295

S. A. Josey, E. C. Kent and P. K. Taylor, 1999: New Insights into the Ocean Heat Budget Closure Problem from Analysis of the SOC Air-Sea Flux Climatology. *J. Climate*, **12**, 2856–2880

G.M. Martin, M.A. Ringer, V.D. Pope, A. Jones C. Dearden and T.J. Hinton, 2006: The physical properties of the atmosphere in the new Hadley Centre Global Environmental Model, HadGEM1. Part 1: Model description and global climatology. *Accepted by J. Climate*

K. E. Trenberth, 1991: Climate diagnostics from global analyses – conservation of mass in ECMWF analyses *J. Climate*, **4**, 707–722

K. E. Trenberth and J. M. Caron, 2001: Estimates of meridional atmospheric and ocean heat transports. *J. Climate*, **14**, 3433-3443

J. Wang, W. B. Rossow and Y.-C. Zhang, 2000: Cloud vertical structure and its variation from 20-yr global rawinsonde dataset. *J. Climate*, **12**, 3041–3056

P.-P. Xie and P. A. Arkin, 1997: Global precipitation: A 17-year monthly analysis based on gauge observations, satellite estimates and numerical model outputs. *Bull. Amer. Meteor. Soc.*, **78**, 2539–2558

X. Yin, A. Gruber and P. Arkin, 2004: Comparison of the GPCP and CMAP merged gauge-satellite monthly precipitation products for the period 1979–2001. *J. Hydromet.*, **5**, 1207–1222

R. Yu, M. Zhang and R. D. Cess, 1999: Analysis of the atmospheric energy budget: A consistency study of available data sets *J. Geophys. Res.*, **108**, 9655–9661

Y. Zhang, W. B. Rossow, A. A. Lacis, V. Oinas and M. I. Mishchenko, 2004: Calculation of radiative fluxes from the surface to top of atmosphere based on ISCCP and other global data sets: Refinements of the radiative transfer model and input data. *J. Geophys. Res.*, **109**, D19105, doi:10.1029/2003JD004457